

ORIENTATIONS OF SPIN AND MAGNETIC DIPOLE AXES OF PULSARS IN THE J0737–3039 BINARY BASED ON POLARIMETRY OBSERVATIONS AT THE GREEN BANK TELESCOPE

P. DEMOREST¹, R. RAMACHANDRAN¹, D. C. BACKER¹, S. M. RANSOM^{2,3}, V. KASPI^{2,3,4}, J. ARONS¹, A. SPITKOVSKY^{1,5,6}

¹Department of Astronomy, University of California, Berkeley, CA 94720-3411, USA

²Department of Physics, McGill University, Montreal, QC H3A 2T8, Canada

Draft version March 15, 2018

ABSTRACT

We report here the first polarimetric measurements of the pulsars in the J0737–3039 binary neutron star system using the Green Bank Telescope. We conclude both that the primary star (pulsar **A**) has a wide hollow cone of emission, which is an expected characteristic of the relatively open magnetosphere given its short spin period, and that **A** has a small angle between its spin and magnetic dipole axes, 4 ± 3 degrees. This near alignment of axes suggests that **A**'s wind pressure on pulsar **B**'s magnetosphere will depend on orbital phase. This variable pressure is one mechanism for the variation of flux and profile shape of pulsar **B** with respect to the orbital phase that has been reported. The response of pulsar **B** to the **A** wind pressure will also depend on the particular side of its magnetosphere facing the wind at the spin phase when **B** is visible. This is a second possible mechanism for variability. We suggest that pulsar **B** may have its spin axis aligned with the orbital angular momentum owing to **A**'s wind torque that contributes to its spindown. Monitoring the pulsars while geodetic precession changes spin orientations will provide essential evidence to test detailed theoretical models. We determine the Rotation Measures of the two stars to be -112.3 ± 1.5 and -118 ± 12 rad m⁻².

Subject headings: pulsars: polarization – radiation mechanism: non-thermal

1. INTRODUCTION

The double pulsar system, PSR J0737–3039, recently reported by Burgay et al. (2003) and Lyne et al. (2004) is likely to unlock many mysteries concerning isolated neutron star magnetospheres and winds as well as the nature of the pulsar emission mechanism. A 22.7-ms pulsar (**A**) and a 2.77 sec pulsar (**B**) revolve about each other in a 2.4h, nearly edge-on orbit. The two stars show interesting and contrasting emission properties. Pulsar **A** exhibits a complex double profile structure. Apart from an eclipse when **A** is behind **B** (with respect to our sight line), this pulsar does not show significant variation in its flux. The flux and profile structure of **B** show remarkable variations as a function of orbital phase (Lyne et al. 2004).

A simple pressure balance calculation leads to the conclusion that the MHD wind of pulsar **A** will suppress a large fraction of the quasi-static **B** magnetosphere. The eclipse duration of pulsar **A** is roughly consistent with this idea (Lyne et al. 2004; Kaspi et al. 2004). Detailed calculations of the **A**-wind/**B**-magnetosphere interactions are required for comparisons with observations (Arons et al. 2004). In this model a bow shock, magnetosheath, magnetopause and magnetotail structures, which are relativistic analogs of solar wind/Earth magnetosphere structures, are established around pulsar **B**.

In this work, we first present polarimetric measurements on these two stars. These observations were conducted at the National Radio Astronomy Observatory⁵ Green Bank Telescope (GBT). After describing our observational setup in §2,

we present our results in §3. Our observations place strong constraints on the geometrical orientation of **A**'s rotation and magnetic axes. We also present our Rotation Measure (RM) measurements for the two stars. In §4 we discuss implications of our polarimetric results within the context of the Arons et al. model.

2. OBSERVATIONS

Observations were performed at the GBT with two backends: BCPM (Berkeley–Caltech Pulsar Machine; see e.g., Camilo et al. 2002) and GBPP (Green Bank–Berkeley Pulsar Processor; see e.g., Backer, Wong & Valanju 2000). The pulsar system was observed at four different frequencies on 2003 December 11, 19, 23, & 24, and 2004 January 1. The bandwidths of our BCPM observations were 96 MHz at 2.2 GHz and 1.4 GHz, and 48 MHz at 0.82 GHz and 0.43 GHz. The GBPP bandwidths were 28 MHz at 2.2 GHz, 1.4 GHz and 0.82 GHz and 11 MHz at 0.43 GHz.

On 2003 December 11 we observed **A** with the GBPP at 1.4 GHz using the published ephemeris (Burgay et al. 2003) and an integration time of 100s. The GBPP provides synchronously averaged, coherently dedispersed profiles that allow calculation of all Stokes parameters.

We first detected and then generated an ephemeris for **B** with the BCPM filter bank total-power data of 2003 December 11. This ephemeris was used for GBPP observations of **B** at 0.82 GHz on 2003 December 19. GBPP observations continued with **A** at 0.43 GHz (briefly), 0.82 GHz and 2.2 GHz and **B** at 0.43 GHz. We also measured a correlated (fully linearly polarized) noise source and observed pulsars with known polarization characteristics (PSR B0656+14 and PSR B0919+06) for calibration purposes. GBPP observations of PSR B1929+10 at 0.82 GHz by I. Stairs for another program on 2003 December 26 were also analyzed for calibration.

3. RESULTS

arXiv:astro-ph/0402025v1 2 Feb 2004

³ Center for Space Research, Massachusetts Institute of Technology, Cambridge, MA 02139

⁴ Canada Research Chair, Steacie Fellow, CIAR Fellow

⁵ KIPAC, Stanford University, P.O. Box 20450, MS 29, Stanford, CA 94309

⁶ Chandra Fellow

⁵ The National Radio Astronomy Observatory (NRAO) is owned and operated by Associated Universities, Inc under contract with the National Science Foundation.

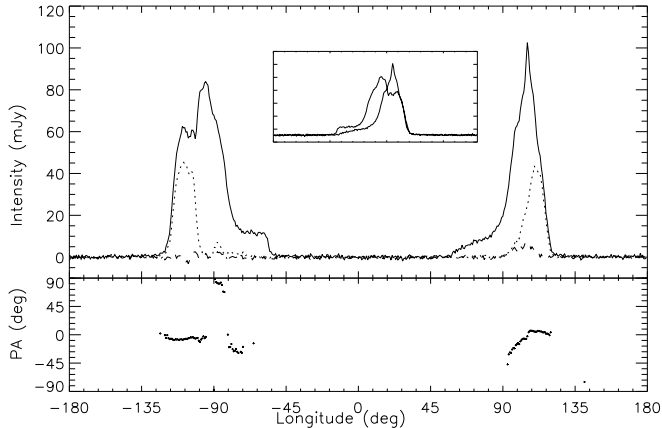


FIG. 1.— Polarization characteristics of J0737–3039A at 0.82 GHz. The inset gives the two portions of the profile ‘mirror-folded’ to show similarity of outer edges. See text for details.

The top panel of Fig. 1 shows the average profile of **A** at 0.82 GHz. The pulsar shows two prominent regions of emission with sharp outer edges, and shallower inner edges. The dotted and dashed lines indicate observed average profiles in linear and circular polarization, respectively. We also show the linear polarization position angle as a function of pulse longitude in the bottom panel of Fig. 1. The longitude region -100° to -70° , and probably the region from $+90^\circ$ to $+105^\circ$, are affected by the presence of quasi-orthogonal polarization modes.

The two emission regions display rough mirror symmetry in both total intensity and linear polarization. We show in the inset on the figure two portions of the profile ‘mirror-folded’ to align the outer edges and emphasize this point. These mirror symmetries suggest to us that these two portions of the pulse arise from traversals of a wide-angle hollow cone at the same magnetic pole rather than the two opposite poles. We have chosen the arrangement of the profile in rotational longitude with steep outer edges in Fig. 1 owing to what is often seen in more compact hollow cones (e.g., Manchester 1996).

Assuming the rotating vector model (RVM; Radhakrishnan & Cooke 1969), we performed a least squares fit to the position angle sweep to obtain the value of the angle (α) between $\vec{\mu}$ and $\vec{\Omega}$ and the angle (β) between the line of sight and $\vec{\mu}$ at closest approach. For this purpose, we ignored the longitudes mentioned above where the PA is likely corrupted by quasi-orthogonal emission modes. The fit was done via a simple grid search in α and β (e.g. Nice et al. 2001). This allowed us to map out χ^2 contours for the solutions, which are plotted in Fig. 2. Two solutions appear, one with $\alpha \sim 5^\circ$ and one with $\alpha \sim 90^\circ$. The large- α solution is unrealistic since it requires a beam opening angle $2\rho \sim 180^\circ$, a geometry where the RVM is likely to be invalid. Furthermore, in this case we would expect to see emission from both magnetic poles, which is inconsistent with the mirror symmetric profile. We favor the small- α solution since it avoids both these problems (see Fig. 3 for a diagram of this geometry). Unfortunately, this leaves β completely unconstrained. Measuring β would give a lower limit on the misalignment between $\vec{\Omega}$ and the orbital angular momentum, since the orbital inclination is well known. However, in the small- α solution $\beta \sim \rho$, so we might

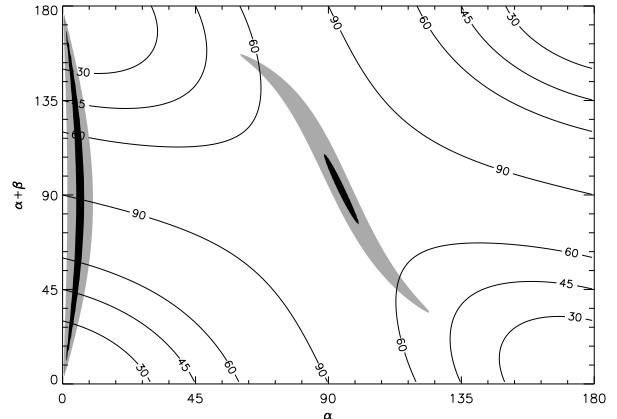


FIG. 2.— χ^2 contours for the RVM fit for **A**. The filled contours represent 1σ and 3σ confidence limits. The line contours show the emission cone opening half-angle ρ for each solution.

expect $\beta \sim 50^\circ$ based on opening angles of other millisecond pulsars.

The characteristics of **B**’s emission are much more complex. Lyne et al. (2004) show that the amplitude and pulse profile vary with orbital phase. Our sensitive data exhibit local maxima in four different ‘windows’ in the orbit (*I* to *IV*⁶). Within the limit of our sensitivity, this 4-window behavior and details of profile evolution within the windows are frequency independent over 0.43 GHz to 1.4 GHz. The signal is seen in almost all other orbital phases at very low flux levels except for a phase range of 30° to 92° , where no flux is detected above 0.1% of that in window *I*. The centroid of the strongest emission (windows *I* & *II*) is $\sim 30^\circ$ prior to when **A** is behind **B**, and the centroid of the phase range when **B** is invisible is $\sim 30^\circ$ prior to when **A** is in front of **B**. Due to the pulse structure evolution, we present the results separately for the four windows in Fig. 4 from our 0.82-GHz observation with the same conventions as in Fig. 1. In window 1 the pulse is polarized at the 15% level and shows orthogonal polarization modes, while in window 2 the polarization is less than a few per cent. A detailed study of individual pulses from **B** and their evolution as a function of orbital phase by Ramachandran et al. (2004) concludes that the subpulse fluctuations are similar to those found in other pulsars of similar period and pulse morphology.

3.1. Rotation Measures

We have measured the RM of the two pulsars from our 0.82 GHz observations. Assuming linearity of polarization position angle sweep within the small bandwidth of 28 MHz, we have derived RM values for pulsar **A** and pulsar **B** from window *I*. We have obtained consistent values of -112.3 ± 1.5 rad m^{-2} and -118 ± 12 rad m^{-2} towards **A** & **B**, respectively. These values are not corrected for ionospheric contributions. Within our measurement errors, we do not see significant orbital phase dependent variations.

4. DISCUSSION

⁶ with the convention followed by Lyne et al. (2004), the ranges of orbital phases (true anomaly) we have taken for the four windows are: $186^\circ - 216^\circ$, $252^\circ - 300^\circ$, $336^\circ - 30^\circ$ and $90^\circ - 132^\circ$, respectively

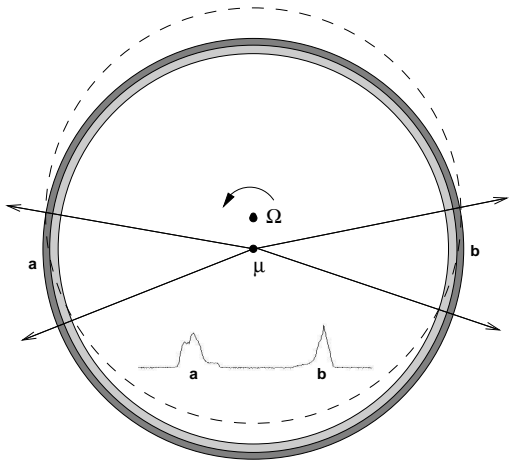


FIG. 3.— The proposed geometry of the emission beam of PSR J0737–3039A, as viewed from above the pole. The grayscale circles indicate the emission cone, centered around the magnetic axis ($\vec{\mu}$). The rotation axis is given by $\vec{\Omega}$. The ‘dash’ line indicates the line of sight trajectory around $\vec{\Omega}$. The radiating vectors from $\vec{\mu}$ are projections of field lines diverging from the pole which nominally give the PA of linear polarization. The two emission regions in the profile are marked as **a** and **b**.

A remarkable feature of both the Lyne et al. (2004) and our GBT observations of J0737–3039B is the dependence of flux and pulse profile, including polarization properties, on orbital phase, but not on radio frequency. We concur in general with Lyne et al. that the variable influence of pulsar **A** on the magnetosphere of **B** is the likely source of the changes. In a companion paper (Arons et al. 2004) we develop a detailed model in which **A**’s MHD wind confines the **B** magnetosphere. We outline this model below, and make connections between observational features that both stimulated the model making and provide directions for future work.

In our model the MHD wind from **A** decelerates through a relativistic bow shock that envelops **B**’s magnetosphere. Between this shock and the boundary of **B**’s closed magnetosphere (**B**’s magnetopause) the shocked **A** wind plasma forms a relativistic hot layer whose optical depth to synchrotron absorption at 500 MHz is at least 100, and may be as high as 5000. This layer (the magnetosheath) is the likely cause of the eclipse of **A** by **B**. In this model we further interpret the faintest region of **B** emission near its superior conjunction as the result of absorption by the same magnetosheath layer that in these phases is between the observer and the pulsar emission region deep within the **B** magnetosphere. In Kaspi et al. (2004) we report that the **A** eclipse is asymmetric with slower flux decrease on ingress and a more rapid recovery on egress. As discussed above the strongest and faintest regions of **B** emission are also asymmetric: both precede times of conjunction by $\sim 30^\circ$. In our model these are attributed to the prograde rotation of **B** that leads to an asymmetric magnetopause and magnetotail. The frequency independence of the eclipse light curve over our observing bands is attributed to sharp boundaries, high optical depths and partial covering in space and/or time.

We favor the interpretation of our polarization observations of pulsar **A** that has the dipole field axis nearly aligned with the spin axis, which itself is oblique to the orbital plane and the line of sight. Pulsar **B** would then experience a significant difference in wind pressure and content around the orbit.

This variable pressure will affect the size of the polar cap and current structure that could lead to the **B** variations.

The **A** wind, asymmetric or not, will produce a propeller torque on **B** owing to **B**’s rotation. This torque contributes to the observed \dot{P} of **B**. In this model the **B** emission results from voltage and e^\pm -avalanche current deep within its magnetosphere similar to that in normal pulsars. The “normalcy” of **B** emission is supported by these polarization observations as well as the single pulse study described elsewhere (Ramachandran et al. 2004).

When we observe pulsar **B**, it presents a different face of its closed and confined magnetosphere to the **A** wind depending on the orbital phase. This variable orientation will also change the **B** magnetosphere and, we suggest, its polar cap and the beamed emission we detect. At this point we cannot distinguish between these two possible sources of modification of the secondary star – variable **A** wind pressure impinging on **B**, and variable **B** internal structure at the rotation phase of observation. They both are seemingly consistent with the frequency independence of the reported phenomena. Both cases will lead to variations in the polar cap size and relativistic current structure of **B**, which will affect the observed flux and its pulse morphology.

In the case of the variable wind pressure, the phase of modulation of **B** is expected to precess around the orbit as the spin of **A** undergoes geodetic precession. Geodetic precession of **B** will have a more complex effect on its internal response to a wind pressure at the spin phase of observation owing to the multiplicity of angles involved.

Our proposed geometry of **A**’s beam will be testable as geodetic precession moves the observer through the cone and into a region of invisibility during the 70-year cycle (Lyne et al. 2004). Is it improbable that we are seeing both pulsars at the same time? We suggest that the **A** wind torque on **B** has aligned pulsar **B**’s spin axis with the orbital angular momentum over time. In this case **B** would need to have its dipole axis at $\alpha \sim 90^\circ$, and therefore we will continue to view **B** independent of geodetic precession. An interesting question is whether the torque of the **A** wind can misalign the dipole while aligning the spin. The full history of the evolution of the system and the dueling magnetospheric winds remains to be written. In its infancy **B** might have had a short spin period and strong magnetic field. If so, then the early wind from **B** could have dominated the **A** magnetosphere and altered its spin and magnetic dipole.

4.1. Summary

Our polarimetric observations indicate that pulsar **A**’s spin and magnetic axes are nearly aligned. This leads us to consider two possible mechanisms for the variability of **B** with orbital phase – (1) a pole to equator asymmetry of the **A** wind, and (2) a rotational asymmetry of the force balance radius of the **B** magnetosphere as it adjusts to the **A** wind. The interaction also contributes to the spin-down torque on the **B** pulsar which may also lead to alignment of the **B** spin and orbital momentum vectors. Geodetic precession will provide an important means of separating the relative importance of the various effects in the coming years. Theoretical calculations are underway to explore these ideas quantitatively.

We thank the GBT staff, and in particular Carl Bignell, Frank Ghigo, Glen Langston and Karen O’Neil, for extensive help with the observations and very useful discussions. We

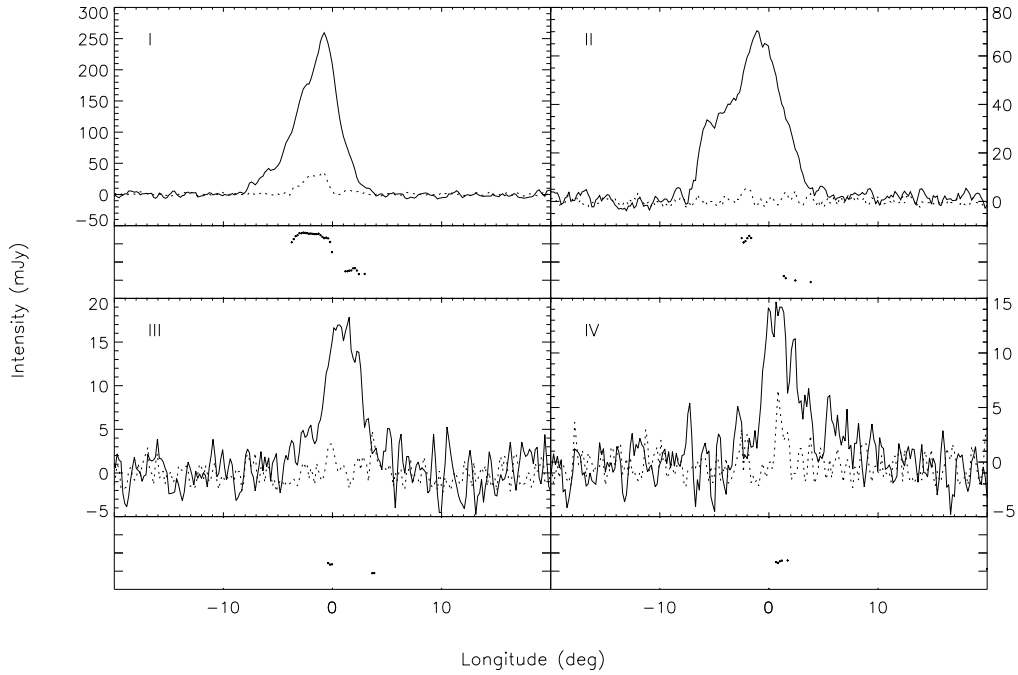


FIG. 4.— Polarization characteristic of J0737-3039B. The four panels give the results for the four orbital phase “windows” see text for details.

thank the initial investigators of the J0737-3039 system for propagating news of this wonderful discovery in advance of publication. We thank the organizers of the 2004 January As-

pen Center for Physics workshop for providing time to present these results that were developed prior to and independently of the meeting.

REFERENCES

- Arons, J.A., Spitkovsky, A., et al. 2004, *ApJ*, in preparation
 Backer, D.C., Wong, T. & Valanju, J. 2000, *ApJ*, 543, 740
 Burgay, M., D’Amico, N., Possenti, A. et al. 2003, *Nature*, 426, 531
 Camilo, F., Stairs, I. H., Lorimer, D. R. et al. 2002, *ApJ*, 571, 41
 Kaspi, V., Ransom, S., Backer, D. C. et al. 2004, *ApJ*, Submitted (astro-ph/0401614)
 Lyne, A. G., Burgay, M., Kramer, M. et al. 2004, *Science*, in press (astro-ph/0401086)
 Nice, D.J., Splaver, E.M. & Stairs, I.H. 2001, *ApJ*, 549, 516
 Radhakrishnan, V., Cooke, D. 1969, *ApL*, 3, 225
 Ramachandran, R., Backer, D. C., Demorest, P. et al. 2004, in preparation